DOI: 10.35840/2631-5084/5545

VIBGYOR ePress

International Journal of
Nanoparticles and Nanotechnology

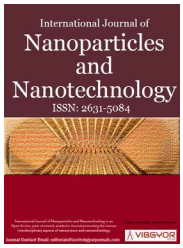

ISSN: 2631-5084

HgS Nanoparticles in Mongolian Medicine Meng-Gen-Wu-Su and its Immunoregulatory Mechanism

***Shikui Wu*[1*], *Nan Zhou*[1], *Chenchen Wang*[2], *Yingze Wang*[2*]**

[1]*College of Pharmacy, The Affiliated People's Hospital, Inner Mongolia Medical University, Hohhot 010059, PR China*

[2]*College of biological science and engineering, Hebei university of science and technology, No.26 Yuxiang street, Shijiazhuang, Hebei, PR China*

Abstract

Mongolian medicine Meng-Gen-Wu-Su (MGWS) is often used to treat autoimmune diseases such as rheumatoid arthritis and psoriasis. How to improve the bioavailability of HgS, and how the immune regulatory mechanism works have not been reported yet. After complex processing technology, the HgS micro-nano particles have been formed in MGWS. The structure and morphology were characterized by XRD, FESEM and TEM. HgS nanoparticles with different particle sizes can be separated by simple differential centrifugation technology. The basic pharmacodynamic effects of HgS nanoparticles were discussed in terms of in vitro dissolution, acute toxicity, immune regulation and apoptotic mechanism of immune cells. The results showed that the maximum tolerance of HgS nanoparticles was more than 36 g•kg-1 (equivalent to 500 times of the clinical dosage), and the dissolution and immune modulation of HgS nanoparticles were size dependent. Through this study, it can be concluded that MGWS can regulate the dissolution dose through the particle size of HgS nanoparticles, and then affect immune cells with a micro-dose of mercury dissolved from HgS nanoparticles.

Keywords

Meng-Gen-Wu-Su, Autoimmune disease, HgS micro-nano particles, Immune regulation, Apoptotic mechanism

Introduction

The traditional Mongolian Meng-Gen-Wu-Su (MGWS) processing method began in the eighteenth century and published in the book of Bi Yong Yao Ji Zhu Pin. The processing methods of all previous dynasties can be classified into three steps, which are descaling, detoxicating and specific drug processing. This processing method is still used today and it can be divided into two kinds, which are the heat process and cold process. Other processing methods have rarely been used or not used at all. The sulfur processing method of Mongolian MGWS is still used until now [1]. MGWS is used to treat rheumatoid arthritis and psoriasis in the rheumatic Immunology Department of Mongolian medicine. Its compound preparation MGWS-18-composition pills have the unique effect of drying "Xieri Wusu". "Xieri Wusu" disease

***Corresponding author:** *Shikui Wu, College of Pharmacy, Inner Mongolia Medical University, Hohhot 010059, PR China; Yingze Wang, College of biological science and engineering, Hebei university of science and technology, No.26 Yuxiang street, Shijiazhuang, Hebei, PR China*

Accepted: June 07, 2024; **Published:** June 09, 2024

Citation: Wu S, Zhou N, Wang C, Wang Y (2024) HgS Nanoparticles in Mongolian Medicine Meng-Gen-Wu-Su and its Immunoregulatory Mechanism. Int J Nanoparticles Nanotech 9:045

mainly refers to psoriasis, rheumatoid arthritis and other autoimmune disease [2]. Chun Lian, et al. conducted a progressive analysis of the clinical application of MGWS-18-composition pills, and the result showed that its application in rheumatology disease accounted for 16.06% and the total effective rate reached 97.5% [3]. EEr, et al. studied the content and dissolution characteristics of mercury in MGWS-18-composition pills, and the result showed that although the mercury content in the compound was 6.385 $mg \cdot g^{-1}$, the dissolution rate was only 0.006-0.009%, and the bioavailability was extremely low [4]. Mongolian medicine has remarkable curative effect on rheumatoid immune diseases with MGWS-18weiwan, but due to low bioavailability, the mercury content in compound is too high. In the background, it is great significant to discuss the metabolite and action mechanism of mercury in the treatment of rheumatic immune disease. The feasibility and mechanism of mercury preparations in the treatment of autoimmune diseases deserve further study.

Through epidemiological investigation of mining workers, Rodriguez, et al. found that mercury exposure did not have a significant impact on workers' antibodies to themselves [5]. The effects of mercury on the human immune system need to be further confirmed. Hultman, et al. studied the relationship between the intake dose of mercury in genetically sensitive mice and the induction of autoimmune diseases and immune complex diseases [6]. A dose of mercury above 15 ng/mL can significantly reduce cell viability ($p < 0.05$). Low dose has different effects on the expression of Th1 and Th2 cytokines, depending on the cell activation pathway In MoAb stimulating cells, the production of IFN-γ, TNF-α and IL-6 is reduced. The dosage was 0.150 and 0.5 ng/mL respectively, increasing the production of IL-10 and IL-4, thereby significantly reducing the Th1/Th2 ratio. However, when heat-killed Salmonella enterica serovar Enteritidis (HK-SE) is stimulated, the ratio of Th1/Th2 is increased due to IFN-γ and IL-10 induction [7]. It can be considered that the immune response of low-dose mercury intake is polarized to Th2 in the absence of inflammation, but it is different from the Th1 polarization reaction caused by salmonella antigen.

Some earlier reports on MGWS focus on the pharmacology and toxicology of the finally prepared medicine [8-10]. One of the important but unanswered problems for the MGWS is its microstructure [11-13]. In contrast to the other works on MGWS, the important effect of the HgS nanoparticles in the MGWS on its medicine efficacy was proposed in our work. At present, more studies suggested that the complex pathogenesis of AID was closely related to Fas/FasL system, which was one of the important ways of apoptosis. MGWS contained the HgS particles with different particle sizes, and its effect on Fas/FasL system in AID had not been reported [14,15]. In this case, the material structure and composition of MGWS was identified, the formation mechanism, and the biological immune effect of HgS nanoparticles was discussed.

Methods

Characterization of MGWS

The phases of the MGWS (Inner Mongolia Mongolian Medicine Co., China) were characterized using powder X-ray diffraction (XRD, Rigaku D/MAX 2400) with Cu-K_α radiation (λ = 1.5406 Å) at a scanning rate of 10 °/min. The size, morphology and structure of the samples were characterized by field emission scanning electron microscopy (FESEM, Hitachi S-4800, with an accelerating voltage of 20 kV), selected area electron diffraction (ED), and high-resolution transmission electron microscopy (TEM, FET TECNAI F30, with an accelerating voltage of 200 kV), respectively. Thermal analysis of the medicine sample was performed under nitrogen atmosphere at a heating rate of 2.5°/min (NETZSCH5 STA 449F3, Germany).

Determination of mercury and free sulfur in MGWS

The content of mercury was titration by thiocyanate, according to the Pharmacopoeia of the People's Republic of China (2015) (the method for cinnabar content determination). The free sulfur was extracted by dimethylbenzene from MGWS. The content of free sulfur was determined according an oxygen flask combustion method.

Autoimmune Regulation of HgS nanoparticles *in vitro*

70 Wistar rats, half male and half female, weighed 180-220g. After one week of adaptive feeding, rats were randomly divided into seven groups: blank, model, positive control (MGWS-18 Weiwan), MGWS, HgS large particle, HgS medium particle and HgS small particle, with 10 rats in each group. According to the routine preparation

method of rheumatoid arthritis model (AA) [16], all rats except the blank group were subcutaneously injected with complete Freund's adjuvant (CFA) 0.1 mL to induce inflammation, while the blank group was injected with saline of equal volume at the same site. When the secondary reaction peak appeared in the model, each group began to administer by gavage. The dosage was 0.520 $g \cdot kg^{-1}$ (the dosage of MGWS-18 Weiwan was converted into 4.626 $g \cdot kg^{-1}$). The drug was administered once a day for 14 consecutive days. To analyze the curative effect of each group of drugs on rheumatoid arthritis. The blank group was given corresponding saline.

Histopathological observation: After blood collection, rats were amputated and fixed in 10% neutral formalin for 2 days. The fixative fluid was replaced once in the middle. After flushing with running water, the rats were decalcified at 37 °C in 8% nitric acid (the thickness of decalcified tissue was 5 mm) for 18-24 h. It was advisable to use needle tip to penetrate the cortex of bone. The decalcified ankle joints were along the sagittal plane. Line is cut in equal volume, flushed overnight with running water, dehydrated and transparent at room temperature, and embedded in wax at 65 °C for preservation. Section and HE staining were performed to observe the effect of the preparation under the microscope and to evaluate the histopathology.

Serum cytokine content: All rats were anesthetized with 10% chloral hydrate (0.3 $mL \cdot kg^{-1}$) at 1 hour after the last administration. Abdominal aorta blood was collected for 30 min and centrifuged for 15 min at 3000 $r \cdot min^{-1}$. Serum was separated and collected. Serum was stored at -20 °C and separated for testing. The concentrations of IL-4, IL-6, IL-10, IL-17, IL-23, TNF-α and IFN-γ in the culture supernatants and the serum and joint tissues lysate supernatants from rats were determined by ELISAs using IL-4, IL-6, IL-10, IL-17, IL-23, TNF-α and IFN-γ kits (Nanjing Jiancheng Bioengineering Institute, China) according to the manufacturer's instructions.

Cell culture and cell viability assay

The RAW 264.7 mouse leukemic monocyte macrophage cell line was maintained in RPMI-1640 medium (Gibco®; Life Technologies) supplemented with 10% (v/v) heat-activated fetal bovine serum (FBS) (Hy Clone; Thermo Fisher Scientific) and 1% (v/v) antibiotic-antimycotic (Gibco®; Life Technologies) at 37 °C in a 5% CO_2 incubator. The cells in the logarithmic growth phase were used for experiments.

96-well plates were inoculated with about 1×10^4 of RAW 264.7 cells per well. After the cells reached 70% confluence, all culture medium was instead of 100 μL of HgS nanoparticles suspension prepared in fresh stock and diluted to an appropriate concentration gradient (0.1 $\mu g \cdot mL^{-1}$, 1 $\mu g \cdot mL^{-1}$, 10 $\mu g \cdot mL^{-1}$, 100 $\mu g \cdot mL^{-1}$, 500 $\mu g \cdot mL^{-1}$). Cells that had not been treated with HgS nanoparticles were used as controls in the experiment. Cells were incubated for 24 or 48 hours at 37 °C in a 5% CO_2 humidified environment. Then 20 μL of the MTS solution (Cell Titer 96 Aqueous One Solution Cell Prolifera, Promega) was added to each well and incubated at 37 °C for 2h. And it was measured at 493 nm by a Multiskan FC microplate reader (Thermo). All of the experiments were carried out in triplicate.

Effects of Fas/FasL expression in RAW 264.7 cells

6-well plates were inoculated with 2 mL of about 2×10^5 of RAW 264.7 cells per well. After the cells reached 70% confluence, all plate culture medium were instead of 1 mL of HgS nanoparticles suspension prepared in fresh stock and diluted to an appropriate concentration (0 $\mu g \cdot mL^{-1}$, 10 $\mu g \cdot mL^{-1}$, 100 $\mu g \cdot mL^{-1}$). Cells were placed in an incubator at 37 °C in a humidified environment of 5% CO_2 in air. After a 24-hours incubation period, the total RNA or the total protein was extracted from the cells. The expression of Fas/FasL gene or its protein was detected by Quantitative real-time PCR or Western blotting.

Statistical analysis

Unless otherwise stated, data values were expressed as mean value ± standard deviation (SD) from three replicates (n = 3). Differences were considered statistically significant at P, 0.05.

Results and Discussion

Structural and morphological characterization of HgS nanoparticles

Figure 1a shows the XRD pattern of the MGWS sample. All the diffraction peaks can be well indexed to the hexagonal phase HgS (cinnabar, JCPDS, No. 6-0256), cubic phase HgS (black, JCPDS,

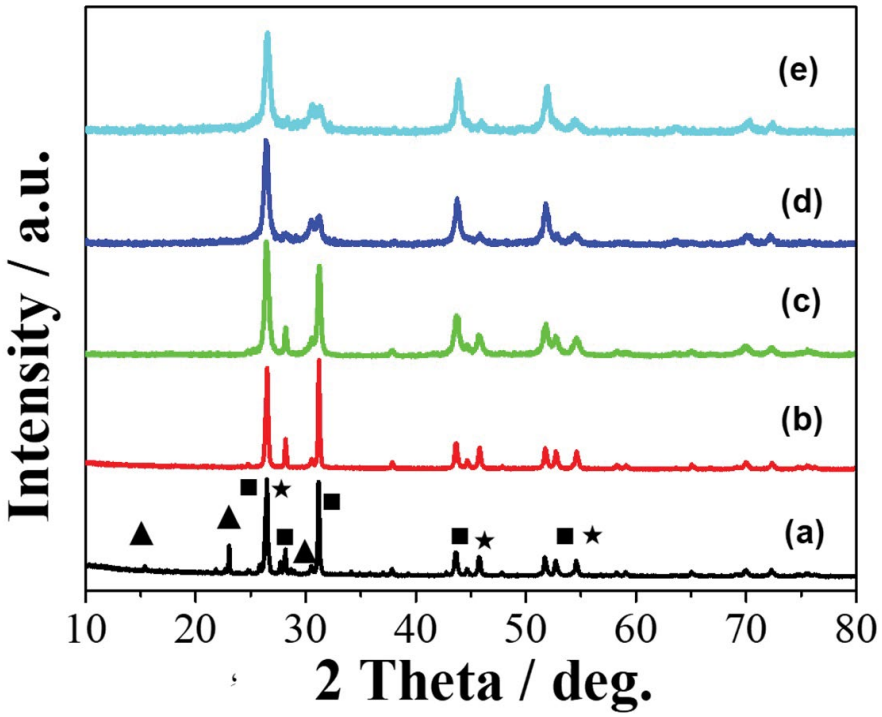

Figure 1: a) The XRD pattern of the MGWS sample; b) The XRD pattern of the MGWS sample after extracting by dimethylbenzene; c) Large (4000-800 nm); d) Medium (800-80 nm) and e) Small (80-20 nm); In the pattern ▲ is the diffraction peaks of hexagonal phase Sulfur; ■ is the diffraction peaks of α-HgS, and ★ is the diffraction peaks of β-HgS.

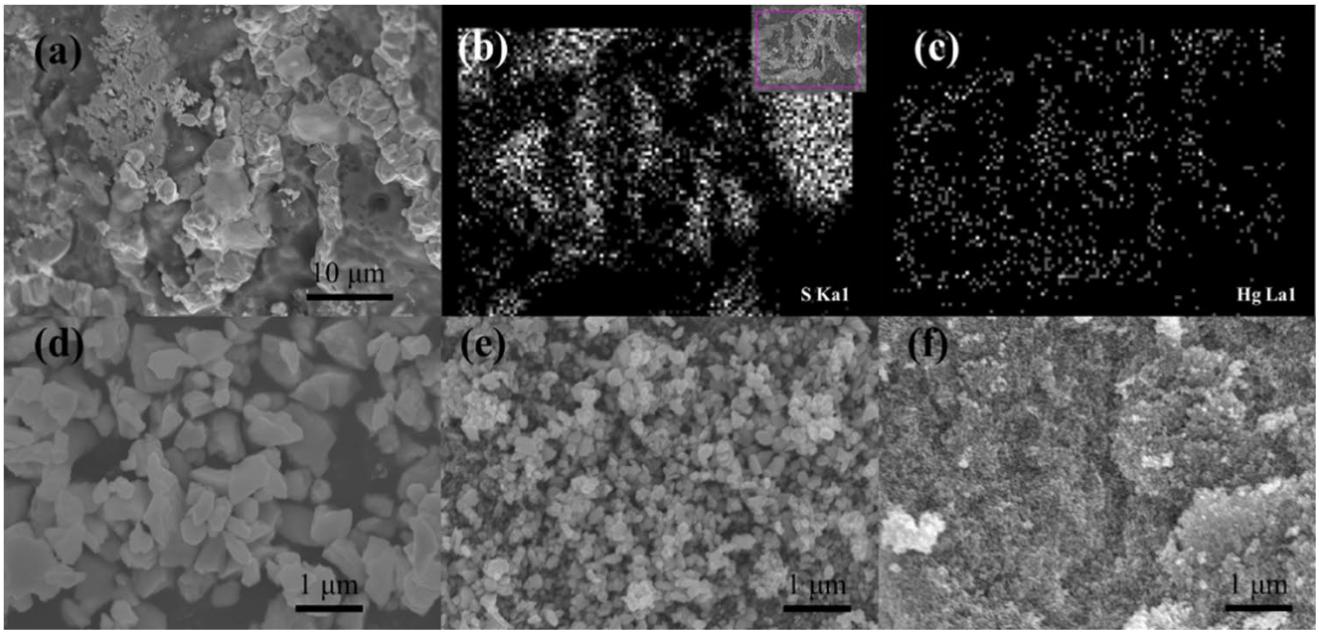

Figure 2: a) The SEM image (Backscattered electron image) of MGWS; b) eElement mapping images of S; c) Element mapping images of Hg; d) Large, e) Medium and f) Small size HgS nanoparticles.

No. 06-0261.), and hexagonal phase Sulfur (S_8, JCPDS, No. 08-0247). Figure 1b shows the XRD pattern of the MGWS sample after extracting by dimethylbenzene. All the diffraction peaks can be well indexed to the hexagonal phase HgS (cinnabar, JCPDS, No. 6-0256, α-HgS), and cubic phase HgS (JCPDS, No. 06-0261, β-HgS), all the peaks of Sulfur disappeared. The result shown that there is a mass

of free Sulfur in the MGWS sample, and they can be extracted by dimethylbenzene, drastically. Figure 1c, Figure 1d and Figure 1e show the XRD pattern of the large (4000-800 nm), medium (800-80 nm) and small (80-20 nm) size HgS nanoparticles separated from MGWS using the mothed in the experience part. All of the samples are the complex of α-HgS and β-HgS.

The section of the MGWS sample was observed by SEM and FESEM, and the result shown in Figure 2. The structure of MGWS sample is irregular under the low magnification (Figure 2a). According to the feature of Backscattered Electron Imaging [17], it can infer that the lighter part of the visual field with high mercury content, and the dark part with high sulfur content. This result is consistent with element mapping images (Figure 2b and Figure 2c). According to the EDS results (Figure S1), rate of mercury to sulfur in samples is not uniform. In the brighter part, mercury content reaches 42.29%, sulfur content is 57.71%, and in the darker part, sulfur content is 94.62% and mercury can't be detected. The Figure 2d, Figure 2e and Figure 2f are FESEM images of the large, medium and small size HgS nanoparticles separated from MGWS using the mothed in our past works [18]. As can be seen from the Figure 2d, Figure 2e and Figure 2f, the size of HgS particles is very uniform, indicating that the differential centrifugation method can effectively separate mercury sulfide nanoparticles from MGWS.

The nanostructure of the medium particle was revealed by TEM. As shown in Figure 3a, all the particles show the irregular size and shapes. Magnified TEM image shows a strong contrast difference in the particles with some darker dots and edge confirms the hollow architecture, which reveals that mass of particles are inlaid in the larger and irregular particles. The HRTEM image inserted in the Figure 3b illustrates that a neighboring crystal domain present on each side across a grain boundary. This implies that the particles are composed of some little single-crystals, and these nanoparticles of HgS embedding in free sulfur inside.

The component analysis of MGWS

The titration of thiocyanate is a common way to detecting the component of mercury or other heavy metals. The experimental result (Table S1) shows that the HgS content is 73.81%, and mercury content is 63.47% with good reproducibility (RSD 0.36%, Recovery 99.45%, and RSD 0.29%).

The TG-DSC and oxygen flask combustion method were used to detect the content of free S element. According the TG-DSC results, the sample of MGWS shows two weight loss (Figure S2a), the first weight loss of 26.0% was observed in the temperature

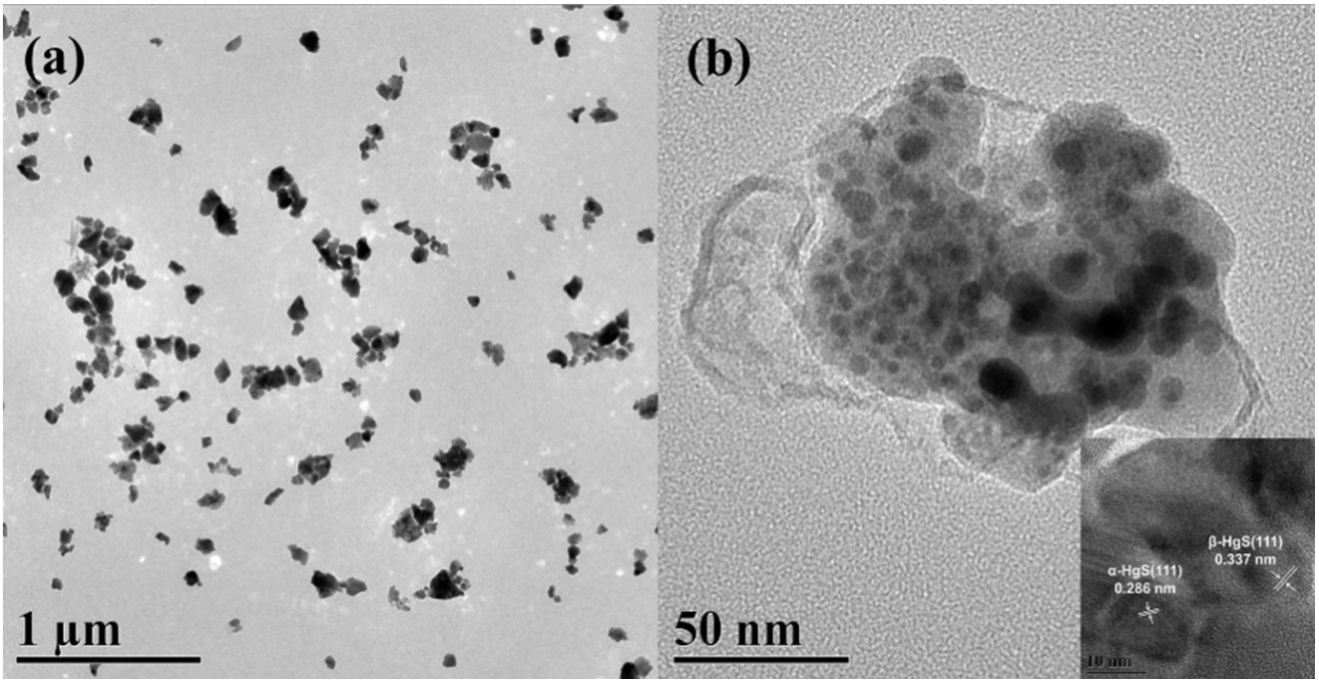

Figure 3: a) The TEM image and b) Magnified TEM image of medium particles, the inset is the HRTEM images.

range from 180 to 260 °C, and the second weight loss of 73.8% occurred between 340 and 420 °C. Combined with the results of DSC, the first weight loss was probably due to the sublimation of the free sulfur, and the second was probably due to the destruction of HgS. Thus, the content of free sulfur is 26.2%, and the HgS is 73.8% in the sample of MGWS. The oxygen flask combustion method shown similar results. For the determination of elemental sulfur, thermal analysis method is more accurate, but their content of α-HgS and β-HgS cannot be determine, respectively. The methods of component analysis need to be developed further more.

The formation mechanism of HgS nanoparticles

According to the literature [19], the MGWS was synthesized from mercury and sulfur (1:2) mixed evenly. In order to remove rust in the mercury, such as HgO, 15 herbal extracts were used to treat mercury before processing. After that, mercury and sulfur are mixed evenly and heated to a melting state. The process requires repeated stirring, and the blue flame is maintained over the sample. Finally, the sample needs to be transferred to an iron container with linseed oil and cooled to room temperature. The heating and cooling process is repeated 21 times. If the section of the processed product is sky blue, it means that the sample has high quality.

Based on the above description, we believe that a series of chemical reactions took place during the processing.

$$Hg + S == HgS \text{ (black)} \quad (1)$$

$$HgS \text{ (black)} \rightarrow HgS \text{ (red)} \quad (2)$$

$$HgS + S == HgS_x \quad (3)$$

$$S + O_2 == SO_2 \text{ (blue flame)} \quad (4)$$

First, in the mixing process, sulfur and mercury react rapidly (Reaction 1) to form black β-HgS particles. In the process of heating and melting, the black β-HgS particles will be transformed into red cinnabar phase (Reaction 2). When the particle size of mercury sulfide is very small, this reaction is easy to occur [20]. Due to excessive sulfur, polysulfides are produced during the reaction, which is beneficial to the phase transformation of HgS. The Figure S3 is the Raman spectra of MGWS. As shown in the Figure, the peaks 257 cm^{-1} and 343 cm^{-1} could be assigned to the *v*(Hg-S) stretching vibration; 483 cm^{-1} could be assigned to S_2^{2-} stretching vibration [13]. The excessive sulfur reacts with oxygen to produce sulfur dioxide, which is used to protect mercury from oxidation (Reaction 3). In addition, repeated stirring plays a key role in the formation of mercury sulfide nanoparticles. In addition, repeated stirring plays a key role in the formation of mercury sulfide nanoparticles.

In our previous work [18], HgS nanoparticles were separated from MGWS, and the size-dependent dissolution of mercury sulfide nanoparticles *in vitro* was verified. The dissolution results of each sample in artificial simulated gastric fluid and artificial intestinal fluid are shown in Table S2. From the results, the mercury dissolution in artificial simulated gastric fluid was significantly higher than that in artificial intestinal fluid. This indicates that pH promotes the dissolution of mercury in mercury sulfide. When the pH is small, the amount of mercury dissolution is large. The dissolution of mercury sulfide particles with different particle size ranges was analysed. It was found that with the decrease of HgS particle size, the dissolution of mercury gradually increased. This fully demonstrates that the particle size of HgS has a certain effect on the dissolution of mercury: The smaller the particle size, the larger the dissolution of mercury. The mercury dissolution of MGWS was between 1 and 2, while the mercury dissolution of MGWS-18 Weiwan was 0.2150 $\mu g \cdot mg^{-1}$, which was significantly higher than that of the MGWS. The results of dissolution of 4# and 5# particles were close to that of the MGWS-18 Weiwan. Here, further toxicity, immune mechanism and apoptotic mechanism of these nanoparticles will be reported. Samples with similar dissolution properties were merged and labeled as large, medium and small particles according to the size range.

The Effect of HgS nanoparticles on the autoimmune system

Maximum Tolerance Dose (MTD) [21]: 80 Kunming mice, weighing 18-22g, half male and half female, were randomly divided into large size particles group, medium size particles group, small size particles group and MGWS group, 20 mice in each group. Before the experiment, the mice were fed with water and fasting for 12 hours at the maximum allowable concentration (0.4 g/mL^{-1}) for 12 hours. Within 12 hours, the mice in the four groups were fed with the suspension with

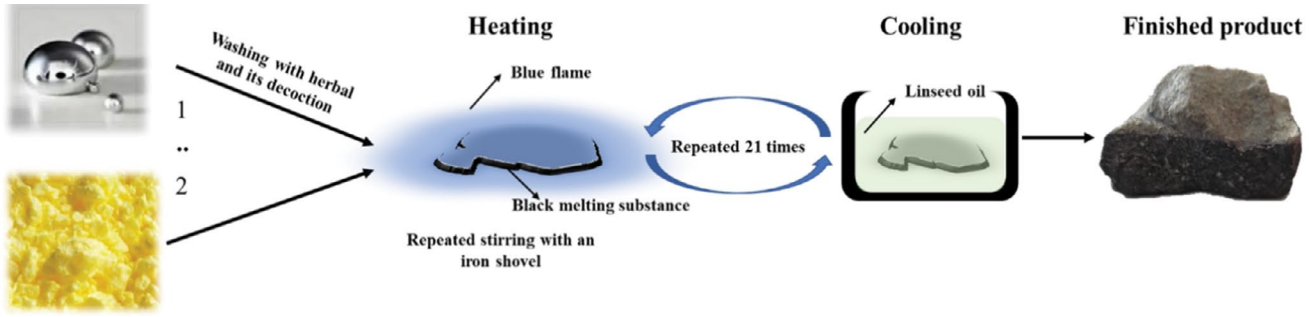

Figure 4: Schematic illustration of the formation process of MGWS.

the maximum allowable concentration (0.2 mL, 10 g^{-1}). All of the four groups mice began to show a decreased activity and quiet phenomenon after administration 30 minutes. After 24 hours, the mice in the four groups resumed normal autonomous activity, drinking water and eating. After 24 hours of administration, the mice in the original medicinal material group of MGWS showed the black color shin and dull hair, which returned to normal the next day. The mice in the big granule group had red feces after administration, while the mice in the other groups had no abnormal feces. During the observation period (14 consecutive days), there was no abnormal food intake and body mass in mice, and no death in all mice. The results showed that the maximum tolerance of mice to large particles, medium particles, small particles and MGWS was more than 36 $g \cdot kg^{-1}$.

Immunomodulatory effect of HgS nanoparticles: After the successful establishment of the model, the joint and the sole of the foot of the rats showed obvious swelling, inflammation, and in severe cases, abscess rupture, toe deformity and other phenomena (Figure S4). One hour after complete Freund's adjuvant (CFA) immunization, swelling appeared in the right hind foot of rats, and obvious redness began to appear at 24 hours. 3-4 days later, acute inflammation occurred in rats, manifested as inactivity, burnout, loss of appetite, redness, swelling, fever and pain at the injection site. 7-8 days later, there was a peak of inflammation, toe swelling and walking restriction in rats. Inflammatory symptoms reached a peak at 14-16 days after CFA immunization. With the prolongation of time, inflammation symptoms decreased slightly. From Table S3 and Table S4, the control group, the medium particles and the small particles group of HgS had different degrees of inhibition on ankle swelling after 12 days of administration ($P < 0.05$). Among them, the control group and the medium particles group of HgS had the best effect, and there was a significant difference compared with the model group ($P < 0.01$).

Histopathological observation: Synovial hyperplasia, pannus formation, destruction of articular cartilage and bone are the main pathological features of rheumatoid arthritis. Pathological sections of ankle joints of rats in each group were observed, and the results were shown in Figure 5. In the blank group, synovial cells were arranged neatly without inflammatory cells, the surface of cartilage tissue was smooth and the space between articular cavity was small; in the AA model group, synovial hyperplasia appeared obviously at the articular joint. With the extension of synovial hyperplasia, the thickened synovium crawled to the cartilage surface, and there were angiogenesis centers in the proliferated synovium, forming pannus. The cartilage was destroyed and a large number of inflammatory cells infiltrated into the articular cavity (Figure 5b); the synovium of the control group was more normal, with a small amount of inflammatory cells infiltrating, the pannus disappearing, and the cartilage tissue was more complete (Figure 5c); compared with the AA model group, the synovium of the original medicinal material group of MGWS and the large particles group of HgS had obvious proliferation and had already been observed. Vascular pannus was formed, inflammatory cells infiltrated seriously, and cartilage tissue was destroyed in varying degrees (Figure 5d and Figure 4e). The destruction of articular cartilage was significantly improved in the medium and small HgS particles groups, and the space between articular cavity was small, and the infiltration of inflammatory cells was reduced (Figure 5f and Figure 4g).

Index of immune organs (spleen and thymus) in rats: Thymus and spleen are two important

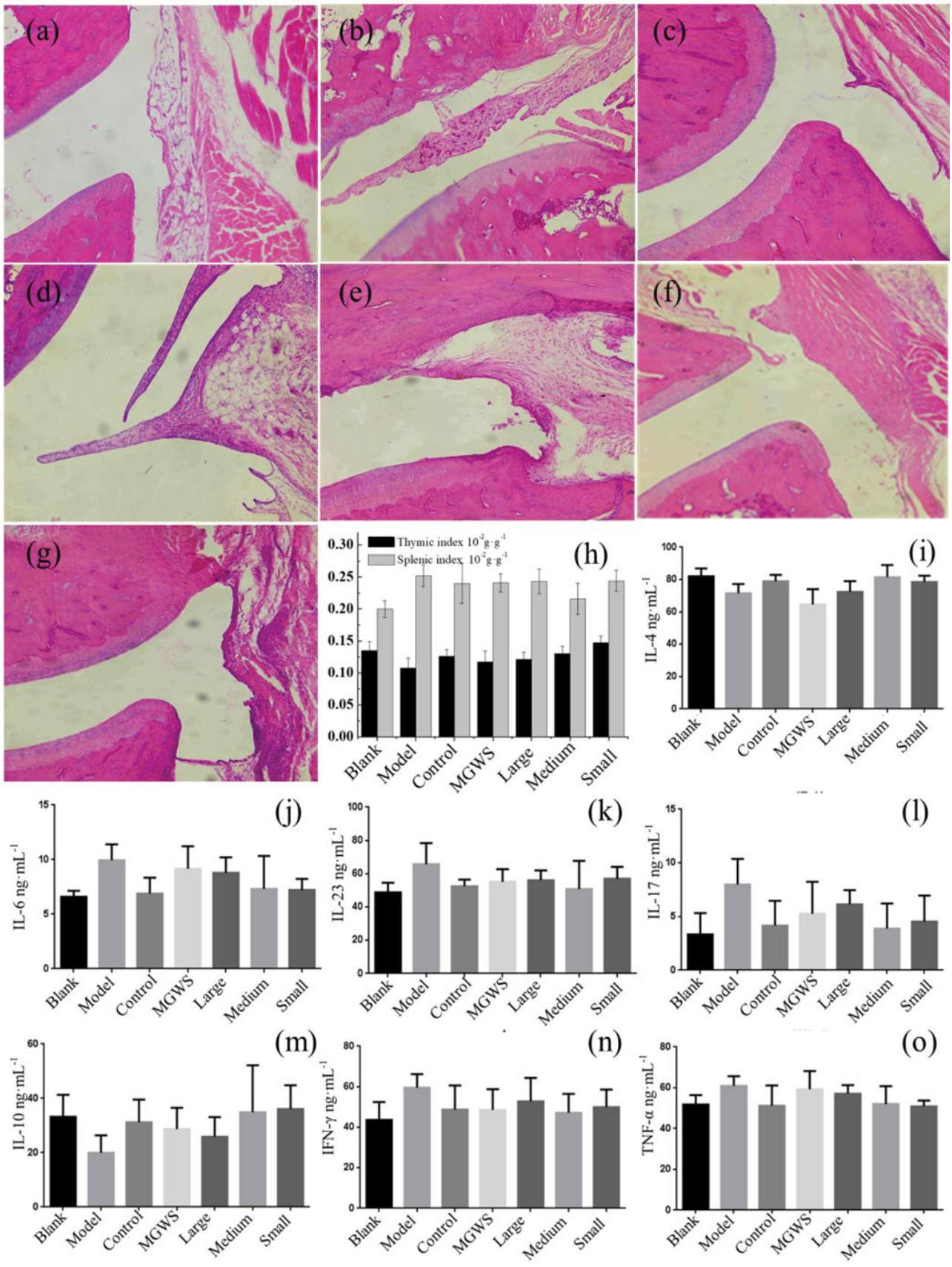

Figure 5: Typical pathological sections of ankle joint of rats in each group after administration (×100): a) Blank; b) Model; c) Control; d) MGWS; e) Large particles; f) Medium particles; g) Small particles; h) Index of immune organs (spleen and thymus) in rats; Levels of serum cytokines in rats (n = 10, x(—)$x \pm S$) i) IL-4; j) IL-6; k) IL-23; l) IL-17; m) IL-10; n) IFN-γ, and o) TNF-α.

immune organs, which can reflect the overall immune function of the body. Thymus belongs to the central immune organ and spleen belongs to the peripheral immune organ. The changes of thymus index and spleen index can reflect the overall immune function of the body [22,23]. As shown in Figure 5h, the thymus index of AA rats was significantly increased in the control group and the medium size particles group of HgS ($P < 0.01$); the spleen index of AA rats was significantly decreased in the medium size particles group of HgS ($P < 0.01$), but there was no significant difference in the other groups. The results showed that HgS particles could significantly improve thymus atrophy and spleen enlargement in AA rats and protect immune organs such as thymus and spleen.

Serum cytokine content in AA Rats: The serum cytokine levels of rats in each group were determined as shown in Figure 5. The levels of IL-6, IL-17, IL-23, IFN-γ and TNF-α in model group were significantly higher than those in blank group, while the levels of IL-4 and IL-10 were lower than those in blank group. The results showed that the control group could significantly reduce the levels of pro-inflammatory factors IL-6, IL-17, IL-23 and TNF-α in serum of AA rats, increase the content of anti-inflammatory factor IL-4 and inhibit the production of inflammatory cells. There was a significant difference between the control group and the model group ($P < 0.05$), indicating that compound MGWS-18 weiwan had a strong immunosuppressive effect. The content of IL-6, IL-17, IL-23 and TNF-α in serum of AA rats was significantly decreased in the medium size particles group of HgS, and the content of anti-inflammatory factors IL-4 and IL-10 was significantly increased compared with the model group ($P < 0.05$). The small size particles group of HgS could also reduce the content of IL-6, IL-17 and TNF-α, and increase the content of IL-10, compared with the model group ($P < 0.05$). There was significant difference between the two groups ($P < 0.05$), which indicated that the medium size and small size particles of HgS could regulate the content of cytokines in serum of AA rats in varying degrees and play an immunosuppressive role in rheumatoid arthritis. However, the large size particles of HgS and the original medicinal materials of MGWS had no such effect.

The effects of HgS nanoparticles on RAW cells

Cytotoxicity of HgS nanoparticles: The growth curves of RAW 246.7 cells were exposed by different

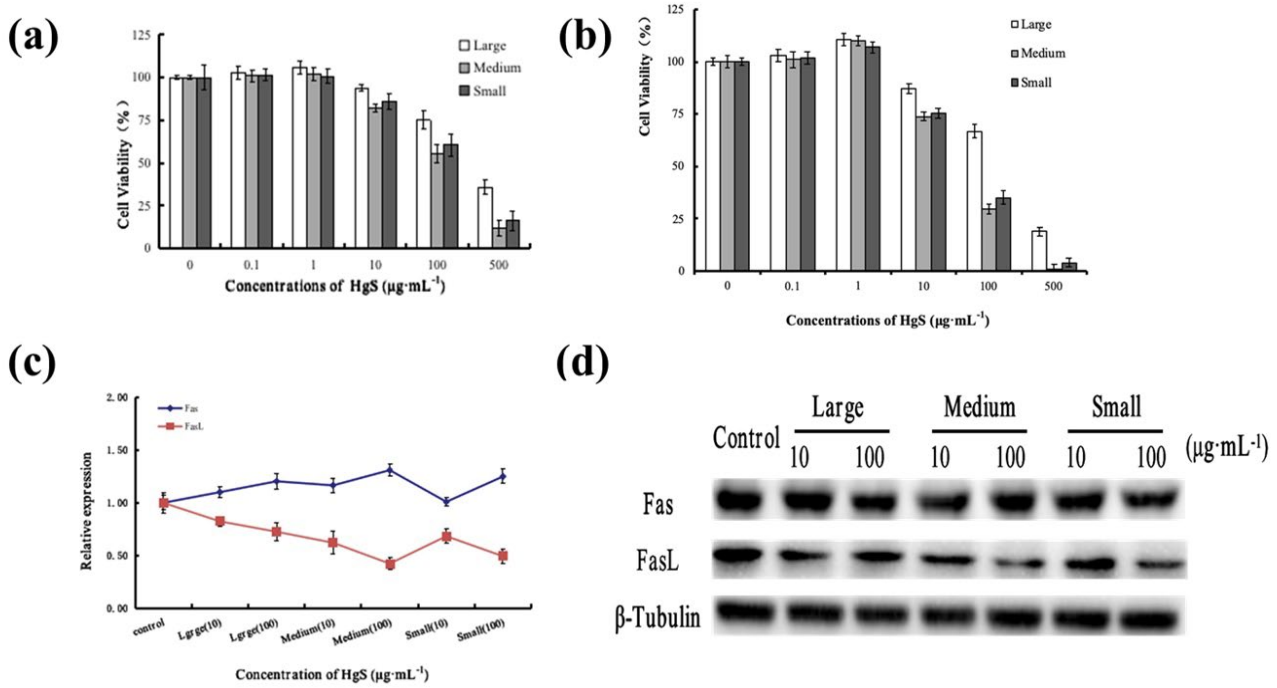

Figure 6: a) The viability of RAW 264.7 cells treated with HgS nanoparticles for 24 h; b) The viability of RAW 264.7 cells treated with HgS nanoparticles for 48 h; c) The effect of HgS nanoparticles on the expression of Fas/FasL genes in RAW 264.7 cells; d) The effect of HgS nanoparticles on the expression of Fas/FasL protein in RAW 264.7 cells.

size and concentration of HgS nanoparticles (Figure 6a and Figure 6b). These results suggest that, the inhibitory effect of HgS nanoparticles on cell viability was enhanced with the increase of exposure concentration. At the same size and concentration, the inhibitory effect of HgS nanoparticles on cell viability was enhanced with the prolongation of the time. Specifically, the cytotoxicity of HgS nanoparticles has concentration effect and time effect. The toxicity of small and medium size HgS was higher than that of large size HgS, and the cell viability has no significant difference treated with small or medium size HgS.

The cell viability of RAW 246.7 cells was more than 50% treated with 100 μg/mL of HgS nanoparticles for 24 hours.

The influence of HgS nanoparticles on the expression level of FasL: Real-time PCR results (Figure 6c) were consistent with Western Blot results (Figure 6d). The HgS nanoparticles had no significant effect on the expression of Fas in RAW 264.7 cells. However, the moderate and low doses of HgS nanoparticles could significantly down-regulate the expression of FasL in RAW 264.7 cells (*, $P < 0.05$), and the effect of medium size HgS nanoparticles was more pronounced than that of small size HgS nanoparticles, which had a clear positive effect on the treatment of autoimmune diseases.

Conclusions

Here, the micro-structure of traditional Mongolian medicine processed product MGWS was characterized by FESEM, TEM, XRD, Raman spectroscopy and TG-DSC analysis. The results showed that a unique microstructure of MGWS with sulfur-coated HgS nanoparticles was formed through the unique processing technology. In the sample, the elemental sulfur was 26.2%. Mercury sulfide was 73.8%, and the HgS nanoparticles with different particle sizes can be separated from MGWS by differential centrifugation. Accordingly, a simple formation mechanism based on polysulfide reaction and repeated stirring are given. Pharmacological experiments showed that the maximum tolerance of HgS nanoparticles was 36 $g \cdot kg^{-1}$, HgS nanoparticles had concentration effect and time effect on the toxicity of RAW 264.7 cells. HgS nanoparticles have size-dependent immunomodulatory effects on AA rats. The moderate and low doses of HgS nanoparticles could significantly down-regulate the expression of FasL in RAW 264.7 cells (*, $P < 0.05$), which had a clear positive effect on the treatment of autoimmune diseases. These results preliminarily explained the scientific of the processing technology of Mongolian medicine MGWS and the material basis role of HgS nanoparticles in its pharmacodynamics. In-depth mechanism research needs to be further strengthened.

Acknowledgements

This work was financially supported by the National Natural Science Foundation of China (81503351, 81760750, 82360824). Development Plan for Innovation Teams in Higher Education Institutions in Inner Mongolia Autonomous Region (NMGIRT2421). Inner Mongolia Autonomous Region Science and Technology Plan (2023YFHH0018). The author also appreciates the support by the 'Central guidance for local science and technology development funds' (Inner Mongolia Autonomous Region Finance Department), the 'Grassland Talent Project of Inner Mongolia Autonomous Region'(CYYC10058), the 'Youth Science and Technology Talents Support Plan' of colleges and universities in Inner Mongolia Autonomous Region (NJYT-18-A09), the Zhiyuan Talent Team of Inner Mongolia Medical University (ZY0120019), Central guidance for local scientific and technological development funds (2022ZY0176).

References

1. Tong H, Hu R, Bao Y, et al. (2013) Exploration of Mongolian Meng-Gen-Wu-Su (Mercury) processing method. Modernization of Traditional Chinese Medicine and Materia Medica (World Science and Technology) 4: 689-696.

2. Bao L, Wu Z, Hong M, et al. (2014) Acute and long-term toxicity study of Mongolian medicine MenkenUsu-18 weiwan. World Science and Technology -- Modernization of Traditional Chinese Medicine 16: 2259-2265.

3. Chun L, Wu L (2013) Current situation of clinical application of Mongolian medicine Menken Usu-18. Journal of Inner Mongolia University of Nationalities (Natural Chinese Version) 3: 319-321.

4. EEr DS, Ba T, Wang X (2011) Mongolian MenkenUsu-18 and the dissolution characteristics of mercury content in research. Journal of pharmaceutical analysis 31: 576-578.

5. Rodriguez L, Florez-Vargas O, Rodriguez-Villamizar

L, Vargas Fiallo Y, Stashenko EE, et al. (2015) Lack of autoantibody induction by mercury exposure in artisanal gold mining settings in Colombia: Findings and a review of the epidemiology literature. J Immunotoxicol 12: 1-8.

6. Hultman P, Enestrom S (1992) Dose-response studies in murine mercury-induced autoimmunity and immune-complex disease. Toxicol Appl Pharmacol 11: 199-208.
7. Hemdan N, Lehmann I, Wichmann G, Emmrich F, Sack U (2007) Immunomodulation by mercuric chloride in vitro: Application of different cell activation pathways. Clin Exp Immunol 148: 325-337.
8. Zhou X, Wang L, Sun X, Yang X, Chen C, et al. (2011) Cinnabar is not converted into methyl mercury by human intestinal bacteria. J Ethnopharmacol 135: 110-115.
9. Huang CF, Liu SH, Lin-Shiau SY (2007) Neurotoxicological effects of cinnabar (a Chinese mineral medicine, HgS) in mice. Toxicol Appl Pharmacol 224: 192-201.
10. Thomas W Clarkson (2002) The three modern faces of mercury. Environ Health Perspect 110: 11-23.
11. Singh SK, Rai SB (2012) Detection of Carbonaceous Material in Naga Bhasma. Indian J Pharm Sci 74: 178-183.
12. Paul S, Chugh A (2011) Assessing the role of ayurvedic 'Bhasms' as ethno-nanomedicine in the metal based nanomedicine patent regime. J Intellect Prop Rights 16: 509-515.
13. Bhowmick TK, Suresh A, Kane S, Joshi A, Bellare J (2009) Physicochemical characterization of an Indian traditional medicine, Jasada Bhasma: Detection of nanoparticles containing non-stoichiometric zinc oxide. J Nanopart Res 11: 655-664.
14. Hendawy N (2017) Pentoxifylline attenuates cytokine stress and Fas system in syngeneic liver proteins induced experimental autoimmune hepatitis. Biomed Pharmacother 92: 316-323.
15. Rodríguez-Frade JM, Guedán A, Lucas P, Martínez-Muñoz L, Villares R, et al. (2017) Use of lentiviral particles as a cell membrane-based mFasL delivery system for in vivo treatment of inflammatory arthritis. Front Immunol 8: 460.
16. Chuu JJ, Hsu CJ, Lin-Shiau SY (2001) Abnormal auditory brainstem responses for mice treated with mercurial compounds: Involvement of excessive nitric oxide. Toxicology 162: 11-22.
17. Lloyd GE (1987) Atomic number and crystallographic contrast images with the SEM: A review of backscattered electron techniques. Mineralogical Magazine 51: 3-19.
18. Wang M, Chen C, Zhou N, Cao Q, Wu S (2018) Extraction, separation, and in vitro dissolution of HgS micro & nano-particles from Mongolian medicine Menken Usu. Chinese Traditional and Herbal Drugs 19: 4513-4519.
19. State administration of Traditional Chinese Medicine (2004) Chinese Materia Medica" editorial board ed. Chinese Materia Medica Mango[M]. Shanghai: Shanghai Science and Technology Press, 2004: 33.
20. Wu SK, Chen CJ, Shen XP, Li G, Gao L, et al. (2013) One-pot synthesis, formation mechanism and nearinfrared fluorescent properties of hollow and porous a-mercury sulfide. Cryst Eng Comm 15: 4162-4166.
21. Hou M, Shi W, Sheng W, et al. (2012) Study on the correlation between different processing methods and acute toxicity of mercury. Journal of Medicine & Pharmacy of Chinese Minorities 1: 63-64.
22. Vas J, Monestier M (2008) Immunology of Mercury. Ann N Y Acad Sci 1143: 240-267.
23. Zahir F, Rizwi S, Haq S, Khan R (2005) Low dose mercury toxicity and human health. Environ Toxicol Pharmacol 20: 351-360.

DOI: 10.35840/2631-5084/5545

Citation: Wu S, Zhou N, Wang C, Wang Y (2024) HgS Nanoparticles in Mongolian Medicine Meng-Gen-Wu-Su and its Immunoregulatory Mechanism. Int J Nanoparticles Nanotech 9:045